International Journal of Automation and Computing 16(4), August 2019, 491-510
DOI: 10.1007/s11633-018-1151-x

Experimental Evaluation of Certain Pursuit and Evasion Schemes for Wheeled Mobile Robots

Amit Kumar[1] Aparajita Ojha[2]

[1] Computer Science and Engineering, Indian Institute of Information Technology Kota, Jaipur 302017, India

[2] Computer Science and Engineering, Indian Institute of Information Technology Design and Manufacturing, Jabalpur 482005, India

Abstract: Pursuit-evasion games involving mobile robots provide an excellent platform to analyze the performance of pursuit and evasion strategies. Pursuit-evasion has received considerable attention from researchers in the past few decades due to its application to a broad spectrum of problems that arise in various domains such as defense research, robotics, computer games, drug delivery, cell biology, etc. Several methods have been introduced in the literature to compute the winning chances of a single pursuer or single evader in a two-player game. Over the past few decades, proportional navigation guidance (PNG) based methods have proved to be quite effective for the purpose of pursuit especially for missile navigation and target tracking. However, a performance comparison of these pursuer-centric strategies against recent evader-centric schemes has not been found in the literature, for wheeled mobile robot applications. With a view to understanding the performance of each of the evasion strategies against various pursuit strategies and vice versa, four different proportional navigation-based pursuit schemes have been evaluated against five evader-centric schemes and vice-versa for non-holonomic wheeled mobile robots. The pursuer′s strategies include three well-known schemes namely, augmented ideal proportional navigation guidance (AIPNG), modified AIPNG, angular acceleration guidance (AAG), and a recently introduced pursuer-centric scheme called anticipated trajectory-based proportional navigation guidance (ATPNG). Evader-centric schemes are classic evasion, random motion, optical-flow based evasion, Apollonius circle based evasion and another recently introduced evasion strategy called anticipated velocity based evasion. The performance of each of the pursuit methods was evaluated against five different evasion methods through hardware implementation. The performance was analyzed in terms of time of interception and the distance traveled by players. The working environment was obstacle-free and the maximum velocity of the pursuer was taken to be greater than that of the evader to conclude the game in finite time. It is concluded that ATPNG performs better than other PNG-based schemes, and the anticipated velocity based evasion scheme performs better than the other evasion schemes.

Keywords: Pursuit-evasion, wheeled mobile robot, proportional navigation, trajectory planning, target interception.

1 Introduction

Pursuit-evasion games are fundamental problems in computer science that provide a suitable platform to study robot motion planning in an adversarial environment. The game in its simplest form typically involves two dynamic agents called “pursuer” and “evader” with opposite interests. While the aim of the pursuer is to catch the evader in minimum possible time, the evader aims at non-interception with the pursuer for maximum possible time. These games have a wide range of applications starting from entertainment computing and cell biology to serious military operations[1–6]. For pursuit-evasion games with two agents, several pursuer-centric approaches have been introduced in the literature. These methods can be broadly classified as artificial intelligence and artificial vision-based techniques[7–11], soft computing based approaches[12–17], line-of-sight (LOS) guidance[18, 19], and proportional navigation guidance (PNG)[20–28] based approaches. Artificial intelligence and artificial vision-based techniques are shown to be effective against a maneuvering evader but these techniques are computationally heavy and not easy to implement in real-world scenarios. Fuzzy logic and neural network based techniques are also used in tracking and intercepting[13, 15, 16]. However, tuning fuzzy/neural based controllers is a time-consuming and complex process because these techniques are usually developed based on trial and error process. Nonetheless, these methods are quite promising and research in these areas is gaining momentum[13, 14, 17].

PNG is one of the most common and efficient approaches used in missile guidance to intercept maneuvering evader. It works on the principle that two moving objects will collide if their direct LOS does not change direction. Classical PNG is well suited to intercept slow maneuvering evaders and has been widely adopted in many applications but does not perform satisfactorily against maneuvering evaders. In view of this, several variants of PNG law have been introduced such as true PNG[24],

Research Article
Manuscript received January 24, 2018; accepted July 21, 2018; published online December 12, 2018
Recommended by Associate Editor Nazim Mir-Nasiri

pure PNG[25], ideal PNG (IPNG)[26] and augmented ideal PNG (AIPNG)[27]. In 2010, a comparative analysis of various PNG methods was conducted and it was shown that the AIPNG method outperformed competing methods[29]. The AIPNG method takes the evader's acceleration into the account as augmented information to efficiently guide the pursuer. The AIPNG method was modified further[29] to deal with high maneuvering evaders. Later, in 2012, a new type of augmented PNG law was introduced known as angular acceleration guidance (AAG) for intercepting high maneuvering evaders[30]. The AAG takes the angular acceleration of the LOS into consideration as augmented information and guides the pursuer to achieve time-optimal interception. Augmented information in terms of evader's acceleration or LOS acceleration helps in directing the pursuer efficiently and time-optimal interception is achieved. However, estimating acceleration is a complex and time-consuming process. In view of this, an anticipated trajectory based proportional navigation guidance (ATPNG) strategy is introduced by the present authors[31]. This strategy does not require any computation for acceleration of the evader rather it is based on a prediction of the future position of the evader. The future position of the evader is estimated using certain angle correction and extrapolation. A few other PNG-based pursuit methods[28, 32, 33] also exist in the literature but cannot be included in this comparison study because of different assumptions and constraints.

While a large number of pursuer-centric schemes are available in the literature, methods in favor of evaders[34–37] are comparatively less explored. Nonetheless, studies on evader-centric problems have gained momentum and various methods have been introduced to avoid interception with pursuer[38–42]. In [38, 39], evasion strategies to avoid intelligent pursuers are described using certain constraints. Three efficient approaches namely classic evasion, random motion evasion, and optical-flow based evasion are evaluated[40]. The evasion strategy using the Apollonius circle is a promising method and has been recently used[41] in pursuit-evasion situations to avoid interception with one or more pursuers. The present authors have also introduced an evasion strategy[42] based on the anticipated velocity of the pursuer. The scheme provides promising results when the environment is free from obstacles, and also when the environment consists of static and dynamic obstacles.

The present study aims at performance evaluation of the above-mentioned pursuit and evasion approaches for wheeled mobile robot applications. Although a large number of pursuit-strategies exist in the literature, to the best of our knowledge, these methods have not been evaluated or compared against available evasion strategies, especially in the wheeled mobile robot set-up. Similarly, very few studies are available on the comparison of evasion strategies against a given pursuit-strategy. Keeping this in view, a comparative study of the performance of PNG-based pursuit-strategies against an evasion strategy is made in the present work. In addition, evasion strategies are also compared against pursuit strategies in terms of the time taken in successfully evading the pursuer and the distance traveled by the pursuer in capturing the evader. Existing PNG based pursuer-centric schemes introduced in the literature are listed in Table 1. Relevant evader-centric schemes are also listed in the same table. The present study involves a single pursuer and a single evader with a maximum speed of the evader limited by the maximum speed of the pursuer. To evaluate pursuit-strategies, we assume that the target/evader is maneuvering. Therefore, only four comparable pursuer-centric schemes namely AIPNG, modified AIPNG, AAG and ATPNG are considered for the study. Further, AIPNG is established to perform better than true PNG, pure PNG and IPNG in [27] and so, these methods have not been considered for the present investigation. For the single evader problem, classic evasion, random motion, optical-flow based evasion, Apollonius circle based evasion and anticipated velocity based evasion are comparable and hence are chosen for the present study. Other schemes either involve multiple pursuers/evaders or impose different constraints.

In order to evaluate the identified pursuit and evasion schemes, the algorithms are implemented on wheeled mobile robots which have the same configuration. The results of hardware implementation are analyzed on the basis of distance traveled/time taken in capture for different initial conditions.

The rest of the paper is organized as follows. In Section 2, objectives of the pursuer and evader are defined in a subspace of the two-dimensional Euclidean space. The pursuer-centric schemes under investigation are described in Section 3, whereas the evader-centric schemes are briefly discussed in Section 4. The experimental results of pursuer-centric versus evader-centric schemes are presented in Section 5. In this section, we also analyze the significance of findings using the student t-test. Finally, in Section 6, conclusions are made based on the comparison that has been carried out.

2 Objectives of the pursuer and the evader

In the present paper, both the players, pursuer and evader, are assumed to be non-holonomic wheeled mobile robots having the same hardware configuration. The maximum maneuvering capacity of each player is normal to its moving direction due to dynamic constraints. It is further assumed that both the players navigate in an obstacle-free workspace W, which is a subset of two-dimensional Euclidean space. Let P, E, V_P and V_E respectively denote the positions and velocities of the pursuer and the evader robots at the current time (say t) as shown in Fig. 1. It is assumed that both players know the

Table 1 Pursuer-centric and evader-centric schemes with their basic assumptions

Scheme	Assumptions
Pursuer-centric schemes	
True PNG[24]	Single pursuer. Single evader. Slow maneuvering evader. The maximum speed of the pursuer is greater than that of the evader. Pursuer and evader can change their acceleration in a bounded range.
Pure PNG[25]	Same as above.
IPNG[26]	Same as above.
AIPNG[27]	Single pursuer. Single evader. High maneuvering evader. The maximum speed of the pursuer is greater than that of the evader. Pursuer and evader can change their acceleration in a bounded range.
Modified AIPNG[29]	Same as above.
AAG[30]	Same as above.
ATPNG[31]	Same as above.
Generalized predictive PNG[28]	Single pursuer. Single evader. Pursuer and evader both move with constant velocities.
Robust PNG[32]	Single pursuer. Single evader. Pursuer and evader both move with constant velocities.
Retro PNG[20]	Single pursuer. Single evader. Non-maneuvering evader moves with constant velocity. The maximum speed of the pursuer is less than that of the evader.
Biased retro-PNG[21]	Same as above.
Biased PNG[22]	Same as above.
Combined PNG[23]	Same as above.
Augmented pure PNG[33]	Single pursuer, single evader. Pursuer and evader both move with constant velocities.
Evader-centric schemes	
Classical evasion[40]	Single pursuer. Single evader. The maximum speed of the pursuer is greater than that of the evader. Pursuer and evader can change their acceleration in a bounded range.
Random motion evasion[40]	Same as above.
Optical-flow based evasion[40]	Same as above.
Apollonius circle based evasion[41]	Single as well as multiple pursuers. Single evader. The maximum speed of the pursuer is greater than that of the evader. Pursuer and evader can change their acceleration in a bounded range. Multiple pursuers involved for faster evader.
Anticipated velocity based evasion[42]	Single pursuer. Single evader. The maximum speed of the pursuer is greater than that of the evader. Pursuer and evader can change their acceleration in a bounded range.
Evasion with integral constraints[38]	Multiple pursuers. Single evader. The integral constraint with the players. Total resources of the pursuers do not exceed that of the evader.
Cell decomposition approach[43]	Multiple pursuers. Single evader. Evader needs to visit several waypoints.
Iterative open-loop scheme[39]	Single pursuer. Multiple evaders. Pursuer is faster than all evaders. Pursuer needs to capture all the evaders.
Generalized Voronoi based evasion[44]	Multiple pursuers. Single evader. Environment is bounded.
Artificial bee colony[45]	Multiple pursuers. Single evader. Evader is avoiding multiple pursuers.
Optimal evasion scheme[46]	Single pursuer. Single evader. Pursuer and evader both move with different but constant velocities. Maneuvering capability of both players is also different.
Evasion scheme by Las Fargeas et al.[47]	Multiple pursuers. Two evaders. Evaders are heterogeneous in terms of speed and sensing capabilities.
Evasion under external flow field[48]	Single pursuer. Single evader. Pursuit-evasion game is played in the presence of external flow field.

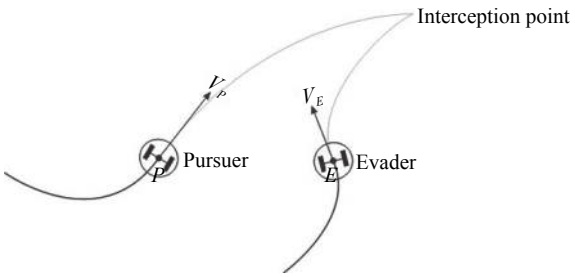

Fig. 1 Sample trajectories of a pursuer and an evader and the interception point

current position of each other at all times but do not know anything about the opponent's moving strategy. It is further assumed that $|V_P^{\max}| > |V_E^{\max}|$, where $V_P^{\max}$ and $V_E^{\max}$ denote the maximum velocities of the pursuer and the evader robots, respectively. This assumption is made to ensure that the game concludes in finite time.

Given the initial positions of the pursuer and the evader, the goal of the pursuer is to minimize the time to capture the evader, while the evader's goal is to maximize the evasion time. P and E are said to be in a collision (P captures E) if $d(P,E) \leq (2r+\varepsilon)$ in a finite time duration, where $d(P,E)$ represents the Euclidean distance in the plane between P and E. r is the radius of the mobile robot (player) and ε is a very small real parameter. The game ends when the above condition is met.

In the following, a brief introduction of all the pursuer-centric schemes considered in the present work is given.

3 PNG law based pursuer-centric schemes

Proportional navigation-based guidance schemes work on the principle that two moving objects fall on a collision curve if their LOS does not change direction in a stable situation. Consider a planar relative motion described by the polar coordinates (R,θ) with the moving coordinate frame located at the pursuer P, as shown in Fig. 2 (a). In this figure, θ is the LOS angle of the pursuer with respect to a reference line (X-axis) and $R = d(P,E)$ where $d(P,E)$ represents the Euclidean distance between the pursuer P and the evader E. e_R and e_θ are the unit vectors in the direction of the LOS and its normal, respectively. Almost all the PNG schemes generate an acceleration command a_c to guide the pursuer. The generated acceleration command a_c helps the pursuer to intercept the evader and is generally computed using the current states of the pursuer and the evader. A brief description of the generated acceleration command in each of the four investigated pursuer-centric schemes is given below.

3.1 IPNG scheme[26]

The IPNG scheme basically relies on the position difference between the pursuer and the evader robots. The acceleration command a_c for the IPNG is given in (1) below:

$$a_c = \lambda L \times \dot{\theta} \tag{1}$$

where λ is the navigation gain and $\dot{\theta}$ is the angular velocity of the LOS. The vector L is the normal direction to the acceleration command and defined in (2) below:

$$L = \dot{R}e_r + R\dot{\theta}e_\theta. \tag{2}$$

A little simplification gives $\dot{R}e_r + R\dot{\theta}e_\theta = \dot{\boldsymbol{R}}$ where $\dot{\boldsymbol{R}}$ is the rate of change of position difference vector between the evader and the pursuer. Hence, the acceleration command for IPNG, which is provided in (1), can be written as $a_c = \lambda \dot{\boldsymbol{R}} \times \dot{\theta}$. The IPNG scheme exhibits the optimal performance against a slow maneuvering evader when $\lambda > 2$ and limit $\dot{\theta} \to 0$.

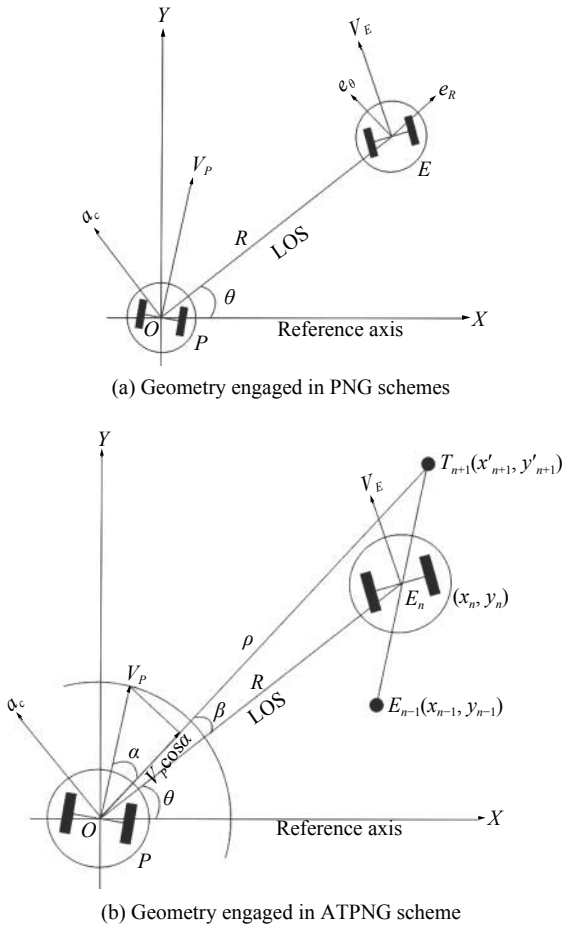

Fig. 2 Schematic diagram for the pursuit and evasion system in two-dimensional space

3.2 AIPNG scheme[27]

The AIPNG technique has been introduced to enrich

proportional navigation guidance to intercept a fast maneuvering target. This scheme improves the IPNG scheme specially against fast maneuvering targets by taking the target's acceleration into account. Therefore, the acceleration command a_c for AIPNG is computed as $a_c = \lambda \dot{\boldsymbol{R}} \times \dot{\theta} + a_E$, where a_E denotes the evader's acceleration. It may be further simplified as follows:

$$(\lambda \dot{\boldsymbol{R}} \times \dot{\theta}) + (a_E - a_c) = 0 \tag{3}$$

$$(\lambda \dot{\boldsymbol{R}} \times \dot{\theta}) + \ddot{\boldsymbol{R}} = 0. \tag{4}$$

Equation (4) is a nonlinear second order differential equation representing the positional difference between the evader and the pursuer. The coefficients of (4) are time and state-dependent scalars, constituting a non-linear system.

The AIPNG scheme shows two major advantages over the IPNG scheme for the interception purpose. First, the AIPNG scheme demonstrates a position-difference equation to compute the error (miss) which is similar to the PD-type control method which is shown in (3) and (4). Second, the position-difference vector $\boldsymbol{R}$ converges to zero for $\lambda > 1$ regardless of the evader's initial position and motion type. The equation $\dot{R}e_r + R\dot{\theta}e_\theta = \dot{\boldsymbol{R}}$ can be converted to $(\ddot{R} - R\dot{\theta}^2)e_r + (R\ddot{\theta} + 2\dot{R}\dot{\theta})e_\theta = \ddot{\boldsymbol{R}}$ after taking differentiation in terms of (4). From this relationship, in combination with (3) and (4), one can derive the following equation.

$$\begin{cases} \ddot{R} - R\dot{\theta}^2 = -\lambda R\dot{\theta}^2 \\ R\ddot{\theta} + 2\dot{R}\dot{\theta} = \lambda \dot{R}\dot{\theta}. \end{cases} \tag{5}$$

Equation (5) represents the motion equation of the pursuer robot guided by the AIPNG scheme for the maneuvering evader exhibits the same interception performance as the performance of IPNG against a slow maneuvering evader. $\dot{\theta}$ approaches to zero for $\lambda > 2$ irrespective of the motion of the evader. On the other side, $\dot{\theta}$ approaches infinity when $\lambda < 2$.

The acceleration command in AIPNG is normal to the relative velocity between the pursuer and the evader[26, 27]. AIPNG is particularly suitable against high maneuvering evaders and produces time-optimal results provided the evader's acceleration is computed correctly. Unfortunately, in real-world scenarios, estimation of the acceleration of a high maneuvering evader is a challenging task.

3.3 Modified AIPNG scheme[29]

The modified version of AIPNG actually improves the smoothness of interception and reduces the chance of missing the target. To provide this smoothness, the scheme guides the pursuer to first minimize the rate of change of the LOS angle and then push the pursuer towards the evader with increased acceleration.

In this guidance scheme, two separate acceleration commands are generated and applied in normal and tangential directions of motion of the pursuer to guide towards the evader. The normal acceleration command is applied to align the pursuer with the LOS and is given by $a_y = a\dot{\theta} + b\sin(\theta - \theta_P)$, where a and b are real-valued constants and θ_P is the angle of the pursuer's moving direction with respect to the reference axis (X-axis). The first component $a\dot{\theta}$ reduces the sensitivity of the pursuer to the changes of the LOS angle and the second component $b\sin(\theta - \theta_P)$ is employed to reduce the deviation angle between the pursuer's moving direction and the LOS. The other acceleration command applied in the tangential direction is given by $a_x = K_p \boldsymbol{R} + K_d \dot{\boldsymbol{R}} + a_{Ex}$, where a_{Ex} is the evader's acceleration component in the frame of reference of the LOS, treating it as the X-axis. K_p, K_d are the gains of the position and the velocity, respectively.

The modified AIPNG scheme guides the pursuer in tracking the evader smoothly by first controlling the rate of change in the LOS angle and then moving towards the evader for a successful interception. Therefore, the chances of missing the evader are minimized but at the cost of high energy consumption and delay in interception because of the large distance traveled by the pursuer as compared to the AIPNG scheme. Nonetheless, both the AIPNG and the modified AIPNG methods perform better than the earlier PN-based interception schemes.

3.4 AAG scheme[30]

Angular acceleration guidance (AAG) is a new type of proportional navigation guidance scheme which is introduced in [30] to intercept high maneuvering evader. This scheme takes the angular acceleration of LOS rather than acceleration of the evader. Conventional proportional navigation based guidance schemes take the LOS rate and the rate of change of the distance between the pursuer and the evader. These schemes including IPNG are most suitable to intercept slow maneuvering evader with almost constant velocity. As discussed above, AIPNG takes augmented information in terms of the evader's acceleration, which is difficult to estimate accurately in the real scenarios, at every point of time to intercept a fast maneuvering evader. The AAG guidance scheme addresses these challenges by taking the double derivative of LOS which is easier to compute online as compared to the acceleration of the evader itself. This scheme guides the pursuer using the following acceleration command:

$$a_c = \frac{\lambda}{2} k(\boldsymbol{R}\ddot{\theta} + 2\dot{\boldsymbol{R}}\dot{\theta} + a_{Py}) - \lambda \dot{\boldsymbol{R}}\dot{\theta} \tag{6}$$

where a_{Py} is the acceleration component of the pursuer in the frame of reference of the LOS and k is a multiplying factor. The angular acceleration of LOS is estimated

using a developed sliding mode observer (SMO) based technique in [30]. The primary benefit of using the SMO-based estimation technique is that the SMO based filter explicitly takes into consideration the effect of noise disturbances and tries to compensate for them using the additional nonlinear switching terms. It is also important to note that the interception in proportional navigation is always successful for the value of $\lambda > 2$ regardless of the initial conditions of the pursuer and the evader[49].

3.5 ATPNG scheme[31]

The working principle of this guidance scheme slightly differs from traditional PNG schemes. This method predicts the evader's trajectory using linear extrapolation and angle correction. The scheme performs two online steps: 1) estimation of the next position on the anticipated trajectory of the evader using linear extrapolation and angle correction and 2) setting the pursuer's acceleration command given by $a_c = [-\lambda K V_P \cos\alpha \times \dot{\alpha}]\cos\alpha$, where α is the angle between V_P and the line segment which connects the pursuer's current position to the next estimated position of the evader (Fig. 2 (b)). The angle α is augmented as $\alpha = \text{sgn}(\alpha) \times \frac{\pi}{2}$ if $|\alpha| \geq \frac{\pi}{2}$ where $\text{sgn}(\alpha)$ represents the sign of the angle α.

The evader's next position after one unit of time is estimated using (7) which is the standard linear extrapolation equation:

$$(x_{n+1'}, y_{n+1'}) = \frac{(t_{n+1} - t_{n-1})(x_n, y_n) + (t_n - t_{n+1})(x_{n-1}, y_{n-1})}{t_n - t_{n-1}} \quad (7)$$

where (x_{n-1}, y_{n-1}), (x_n, y_n) and (x_{n+1}, y_{n+1}) are the evader's positions at the time t_{n-1}, t_n and t_{n+1}, respectively. These schemes are applicable to the non-holonomic wheeled mobile robot because it is possible to estimate the future position of the pursuer robot after one unit of time accurately. Moreover, the next position estimation using linear (7) is a lightweight computation as compared to the computation of the acceleration of the evader or of the LOS angle. The basic difference in the geometry engaged in this scheme and other schemes is shown in Fig. 2. A brief overview of all these PNG-based pursuer-centric schemes is given in Table 2.

The above described four pursuer-centric schemes AIPNG, modified AIPNG, AAG, and ATPNG have been considered for performance evaluation against five different evader-centric schemes. The investigated evader-centric schemes are briefly discussed in the following section.

4 Evader-centric schemes

The first three evasion techniques are modeled for a constant speed evader and direction of motion of the

Table 2 Summary of the investigated pursuer-centric schemes

Scheme	Assumptions and intuition behind the techniques
All four investigated schemes in favor of the pursuer are applicable only with single pursuer and single evader. Assumptions: 1) The maximum speed of the pursuer is greater than that of the evader to conclude the game in finite time. 2) Both robots can see each other at all the times during the operation. This assumption is achieved using the ultrasonic sensors.	
IPNG	Intuition: IPNG scheme relies on the position between the pursuer and the evader. The scheme pushes the pursuer toward the current position of the evader to continuously reduce the distance between these two objects. Remark: Intercept efficiently only if the evader is slow maneuvering.
AIPNG	Intuition: AIPNG relies on the current position as well as the acceleration of the evader. Hence this is just an improvement of the IPNG. Remark: This is able to intercept a fast maneuvering evader also.
Modified AIPNG	Intuition: This scheme first set the pursuer's moving direction in the LOS angle and then push the pursuer directly towards the evader for the interception. Therefore, the chances of missing the evader are minimum even if the evader is a fast maneuvering.
AAG	Intuition: Inspired by the modified version of AIPNG, this scheme sets the pursuer in the direction of the evader by taking the acceleration of the LOS angle. Remark: The computational cost of the LOS angle acceleration is less than the computational cost of the evader itself. Hence the AAG scheme performs usually better than conventional PNG based guidance schemes.
ATPNG	Intuition: This technique is slightly different from the traditional PNG techniques. ATPNG actually moves the pursuer towards the estimated future position of the evader after one unit of time. The future position is estimated using linear extrapolation and the guidance command for the pursuer is based on proportional navigation. Remark: This scheme works efficiently only with non-holonomic constraints in which the next position can be accurately estimated.

evader is controlled by an angular velocity command $\dot{\theta}_E$. The evaders have been modeled as self-propelled steered agents with strategy-based motion control. Assume that θ_P and θ_E are the arguments of the positions of the pursuer and the evader respectively (in polar coordinates). The dynamics of the pursuer and the evader are shown in Fig. 3.

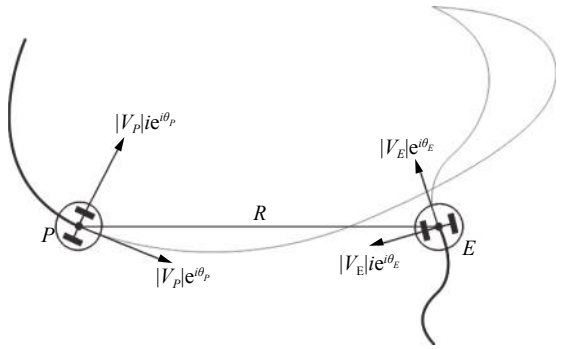

Fig. 3 Sample trajectories of a pursuer and an evader. $|V_P|\,e^{i\theta_P}$, $|V_P|\,ie^{i\theta_P}$, $|V_E|\,e^{i\theta_E}$ and $|V_E|\,ie^{i\theta_E}$ are representing the velocities in the tangential and normal directions of pursuer and evader, respectively.

Let

$$\begin{cases} \dot{P} = |V_P|\,e^{i\theta_P} \\ \dot{E} = |V_E|\,e^{i\theta_E} \end{cases} \tag{8}$$

where $|V_P|$ and $|V_E|$ denote constant speeds of the pursuer and the evader with $|V_P| > |V_E|$. The angular velocity command denoted by $\dot{\theta}_E$ in classical, random motion and optical-flow based evasion techniques are defined as follows[40].

4.1 Classical evasion[40]

The method is based on (9) to compute the value for $\dot{\theta}_E$.

$$\dot{\theta}_E = -\eta \left\langle \frac{R}{|R|}, ie^{i\theta_E} \right\rangle \tag{9}$$

where η is a constant gain. Intuitively, the classical evasion scheme tries to align the velocity vector of the evader with the relative position vector R. This is one of the simplest evasion schemes which demands less computing requirement and shows reasonable efficiency with non-holonomic constraints. It has also been shown in [40] that the evader using classical evasion scheme is captured in finite time in Euclidean space subject to $|V_P^{\max}| > |V_E^{\max}|$ for every initial condition.

4.2 Random motion evasion[40]

In this scheme, the evader moves piecewise linearly with turns every Δ time unit and the value of $\dot{\theta}_E$ is selected uniformly randomly between $[-h, h]$ at every turn. h is a real-valued constant used to calibrate the computed value of $\dot{\theta}_E$ with the angle by which the evader robot will turn. The maximum allowed turning for both robots is with the angle $\frac{\pi}{2}$ clockwise and anti-clockwise directions. In our case, the range of the constant h is $0 \le h \le 45$. At $h = 45$, the evader robot turns by $\frac{\pi}{2}$ while at $h = 0$ the robot moves linearly.

The random motion behavior of any object lets the object move around the canvas along a random path. Although the trajectory generated with this behavior appears to be random but in reality the motion is pseudo-random because of the limiting factor h. Moreover, the motion of the evader does not change if the value of h is the same at every unit of time. Pais and Leonard[40] have done Monte-Carlo simulations and analytical calculations to study the performance of random motion evasion against various pursuit strategies.

4.3 Optical-flow based evasion[40]

In this scheme, $\dot{\theta}_E$ is calculated using (10) which is given below:

$$\dot{\theta}_E = -\eta \tan^{-1}(\dot{\theta}) \tag{10}$$

where $\dot{\theta}$ is the rate of change in the complex argument of the relative position vector, i.e., $\dot{\theta} = \frac{-1}{|R|^2}\left\langle R, i\dot{R}\right\rangle$. Intuitively, in this evasion strategy, the evader reacts to the changes in the argument of the relative position vector R. It can be noticed that this scheme tries to keep the relative position vector parallel to the pursuer.

Apart from these three evasion techniques, a well-known Apollonius circle-based evasion strategy has been recently used in [41] and is also selected for the present study. In this scheme, the evader plans its motion by generating an Apollonius circle to prolong the capture. A brief description of the scheme is given below[41].

4.4 Apollonius circle based evasion[41]

In this scheme, the evader forms an Apollonius circle whose foci are the positions of the pursuer and the evader at the time t (see Fig. 4). D is the set of points that generate the circle such that $W = \left|\frac{PD}{ED}\right| = \frac{V_P}{V_E}$. The radius AO and the center O of the generated circle are defined as $\frac{W\sqrt{(x_1-x_2)^2+(y_1-y_2)^2}}{|1-W^2|}$ and $\frac{(x_1 - W^2 x_2 1 - W^2)}{y_1 - W^2 y_2 1 - W^2}$, respectively. A triangle PAB in Fig. 4 called critical triangle is also determined by the evader based on the current position of the pursuer P. Line segments PA and PB are the tangents from the point P to the generated circle. The evasion method to prolong the capture for the maximum possible time works

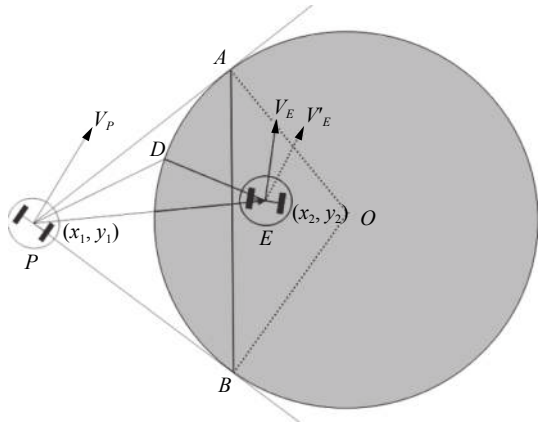

Fig. 4 An Apollonius circle with radius AO and the center O is formed by the evader based on the current positions of the pursuer and the evader.

as follows.

Given an initial velocity of the evader, a random motion evasion technique is used to compute the next velocity vector V'_E for the evader (Fig. 4). If the ray emerging from E in the direction of V'_E does not intersect the triangle PAB, then the evader moves with the new velocity vector V'_E for one unit of time and again uses the random motion evasion strategy to compute the new velocity to be applied after one unit of time. Otherwise, the evader computes V'_E by repeated application of random motion evasion technique until a safe motion direction is decided.

In addition to the above-mentioned strategies, an evasion strategy has also been recently introduced based on trajectory anticipation of the pursuer[42]. The scheme is briefly described here.

4.5 Anticipated velocity based evasion[42]

In this evasion scheme, the evader anticipates the pursuer's future motion direction in order to plan its own moving strategy. More specifically, the evader estimates the next position of the pursuer by assuming that the pursuer would move towards the evader on a quadratic curve joining the points (x_0, y_0), (x_1, y_1) and (x_2, y_2) as shown in Fig. 5, where (x_0, y_0) are the Cartesian coordinates of the pursuer's previous position (before a time unit). The predicted motion path is modeled using a

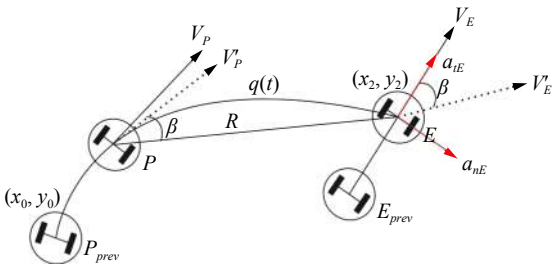

Fig. 5 Pursuer's future trajectory estimation at time t using polynomial interpolation

quadratic polynomial interpolant $q(t)$ to the positions (x_0, y_0), (x_1, y_1) and (x_2, y_2) at the three consecutive time instances t_0, t_1 and t_2.

Now, the velocity V'_P of the pursuer is anticipated by computing the tangent to the curve $q(t)$ at the point (x_1, y_1) at the current time t. Using this, two separate acceleration commands provided in (11) and (12) are generated. The first acceleration command is in the normal direction of the evader's body axis which is denoted by a_{nE} (Fig. 5) and given in (11). This command rotates the evader in a safe direction away from the pursuer and is expressed as

$$a_{nE} = \begin{cases} w\cos\beta n_E, & \text{if} \quad \beta \leq 0 \\ -w\cos\beta n_E, & \text{if} \quad \beta > 0 \end{cases} \tag{11}$$

where w is a real-valued constant, n_E is the unit vector in the normal direction to the evader's body axis and β is the angle between V'_P and the vector $(x_2, y_2)-(x_1, y_1)$. The new velocity vector of the evader after rotation is denoted by V'_E (Fig. 5). The second acceleration command generated by this method is denoted by a_{tE} and provided in (12). This command is in the tangential direction of the evader's body axis and is expressed as below:

$$a_{tE} = |V_E^{\max}|\,\psi n_T \tag{12}$$

where n_T is the unit vector in the direction of the evader's body axis and ψ is a constant of proportionality with the relation $\psi = \dfrac{1}{|a_{nE}|}$. The tangential acceleration command a_{tE} manages the evader's linear velocity from zero to $V_E^{\max}$. In essence, a_{nE} and a_{tE} guide the evader to run away from the pursuer by updating the evader's velocity vector after each unit of time. A sense of the working principle of evader-centric schemes is provided in Table 3.

5 Performance evaluation

In this section, interception performance of pursuer-centric schemes versus evader-centric schemes is evaluated in terms of how quickly a pursuer can intercept the evader and how long an evader is able to avoid interception.

5.1 Experimental setup

The game is played in an open and obstacle-free planar environment. Two non-holonomic wheeled mobile robots of the same configuration are fabricated as the pursuer and the evader (Fig. 6). Each robot is equipped with Arduino Mega as the controller board and has eighteen equispaced sonar sensors on its outer surface to sense the opponent player in the environment. The initial distance between the players was taken using the range of

Table 3 Summary of the investigated evader-centric schemes

Scheme	Assumptions and intuition behind the techniques
All five investigated schemes in favor of the evader are applicable only with a single evader. Assumptions: 1) Pursuer and evader can change their acceleration in a bounded range. 2) Both robots can see each other at all the times during the operation. This assumption is achieved using the ultrasonic sensors.	
Classical evasion	Intuition: This evasion scheme tries to keep the evader's moving direction aligned with the relative position vector R.
Random motion evasion	Intuition: The evader moves straight for one unit of time and then turns arbitrarily in any direction.
Optical-flow based evasion	Intuition: This scheme responds to the change of LOS angle between the pursuer and the evader. It actually tries to make the evader move parallel to the pursuer by reducing the rate of change of the LOS angle.
Apollonius circle based evasion	Intuition: In this scheme, the evader moves in a random direction after each moment of time. Every time, the new moving direction for the evader is chosen randomly by satisfying some constraints imposed by the generated Apollonius circle.
Anticipated velocity based evasion	Intuition: This evasion scheme first anticipates the future trajectory of the pursuer. Then the scheme rotates and accelerates the evader in a safe direction using two separate guidance commands.

(a)

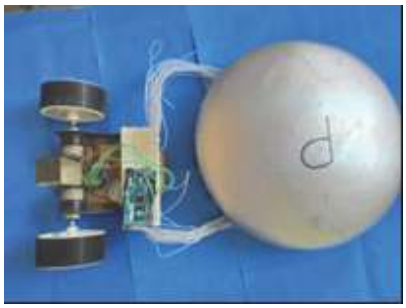

(b)

(c)

Fig. 6 Image of both the fabricated robots: (a) Pursuer robot and (b) its circuit. Sonar sensors mounted on the surface are connected with Arduino Mega through white wires (c) Evader robot is similar.

the sensors so that they can sense each other at all times during the game. The code was written in C^{++} using player/stage simulator and then transfer to the real controllers of both the robots.

5.2 Initial parameters settings

The start positions and initial motion directions of the pursuer and the evader robots are kept the same for all the schemes for comparison. Starting with a distance of 1.5 m between players, the maximum velocity of the pursuer robot is taken as δ times the evader's maximum velocity, i.e., $V_P^{\max} = \delta V_E^{\max}$ where $\delta > 1$. The selection of the parameter value δ plays an important role in the performance of the pursuer-centric schemes. A small value of δ (say $\delta = 1.1$) limits the maximum velocity of the pursuer almost equal to the evader's maximum velocity and therefore the pursuer takes more time and traverses a large distance to intercept the evader. It has also been observed that a large value of δ (say $\delta > 1.5$) accelerates the pursuer resulting in missing the rendezvous point. Therefore, the value δ is taken to lie in the range [1.2, 1.5]. Accordingly, velocities are set as follows. ${V_P}^{\max} = 0.9$ m/s and $V_E^{\max} = 0.7$ m/s by considering the value of $\delta = 1.3$.

5.3 Experimental results

Interception time and distance traveled by the players have been noted to evaluate the performance of the pursuer-centric and evader-centric schemes. A series of experiments are conducted to evaluate the performance of each pursuer's scheme against each evader's scheme by initially taking the value of $\delta = 1.3$ and $ini\_dis = 1.5$ as mentioned above. Fig. 7 shows the performance of all evader-centric approach against each pursuer-centric approach. It can be observed in Fig. 7 that anticipated velo-

city-based evasion scheme performs better among all evasion schemes. On the other side, it can also be observed that the anticipated trajectory based pursuer scheme is able to intercept fastest while AIPNG method shows the worst performance. Fig. 8 shows the quantitative results of all pursuer-centric schemes against each evader-centric scheme. Fig. 9 shows the comparison in terms of interception time.

Comparative performance is also measured for different initial distance values between the players, i.e., $ini\_dis \in \{1.5, 2, 2.5, 3\}$ for validation of the results. Results show the consistency in performance and are listed in tabular form in Appendix A. Further, results of the actual path traveled by the pursuer and the evader robots for the initial conditions $ini\_dis = 1.5$ and $\delta = 1.3$ are also shown in Figs. 10–14 as a representative case.

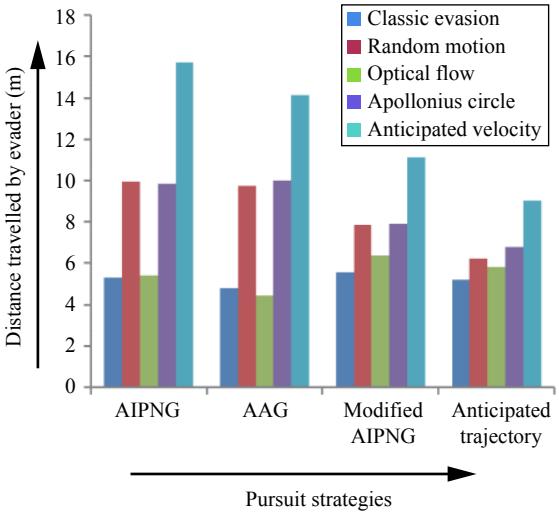

Fig. 7 Performance comparison of all evader-centric schemes against each pursuer-centric scheme

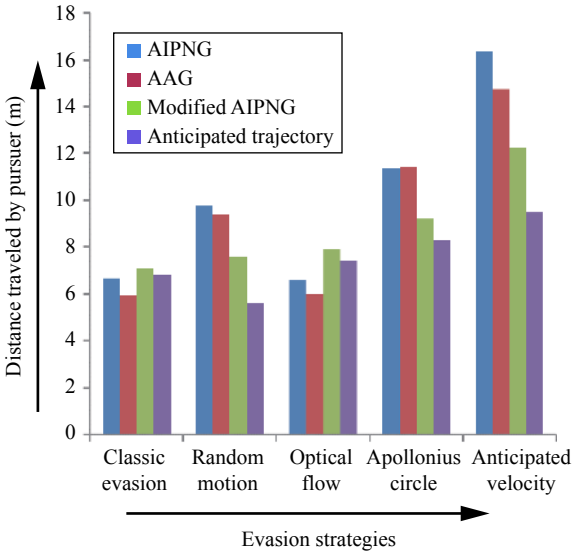

Fig. 8 Performance comparison of all pursuer-centric schemes against each evader-centric scheme

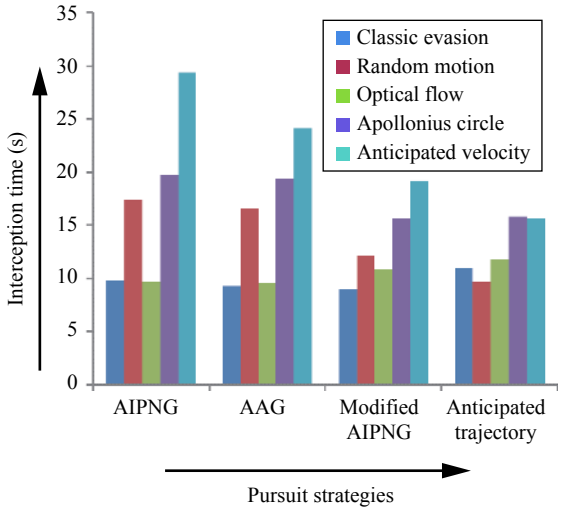

Fig. 9 Performance comparison in terms of interception time

5.4 Result analysis

5.4.1 Pursuer-centric schemes

The AIPNG and AAG schemes behave in nearly the same way while modified AIPNG and anticipated trajectory-based PNG schemes show better interception capabilities especially in the case of a high maneuvering evader. The main drawback of the AIPNG and AAG schemes is a loss of accuracy in estimating the rendezvous point possibly due to inaccurate estimation of the evader's acceleration in real time. Modified AIPNG scheme constantly works to align the pursuer on the LOS so that the pursuer finds it easy to hit the evader. However, it also results in a long interception time. It may be observed that the anticipated trajectory-based PNG scheme is able to intercept the evader quickly, without missing the rendezvous point especially in the case of a high maneuvering evader because this scheme guides the pursuer to follow the LOS while moving towards the estimated future position of the evader for an interception.

5.4.2 Evader-centric schemes

On the opponent side, classic and optical-flow based evasion schemes behave in nearly the same way because both schemes react to the changes in the relative position vector. The main drawback of these schemes is they are not able to maneuver fast when the pursuer follows the evader in the direction of LOS. Random motion and Apollonius circle-based evasion schemes are able to prolong the capture as compared to the classic and optical-flow based evasion schemes. Random motion evasion relies purely on the random turn at every unit of time-based on uniform distribution and its performance is quite similar to the Apollonius circle-based evasion. The anticipated velocity-based evasion scheme uses polynomial interpolation to predict the trajectory of the pursuer and moves in the safe direction to avoid interception as

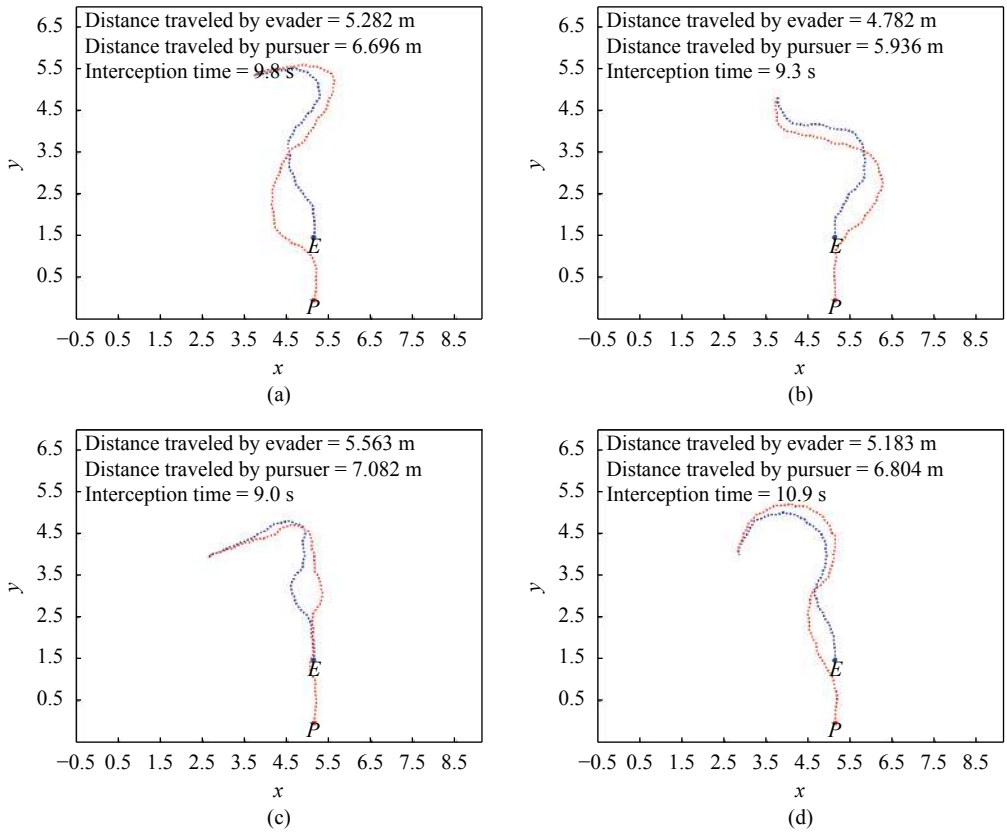

Fig. 10 Interception performance of different pursuer-centric schemes: (a) AIPNG; (b) AAG; (c) Modified AIPNG; (d) Anticipated trajectory based PNG. The evader is guided by the classical evasion scheme.

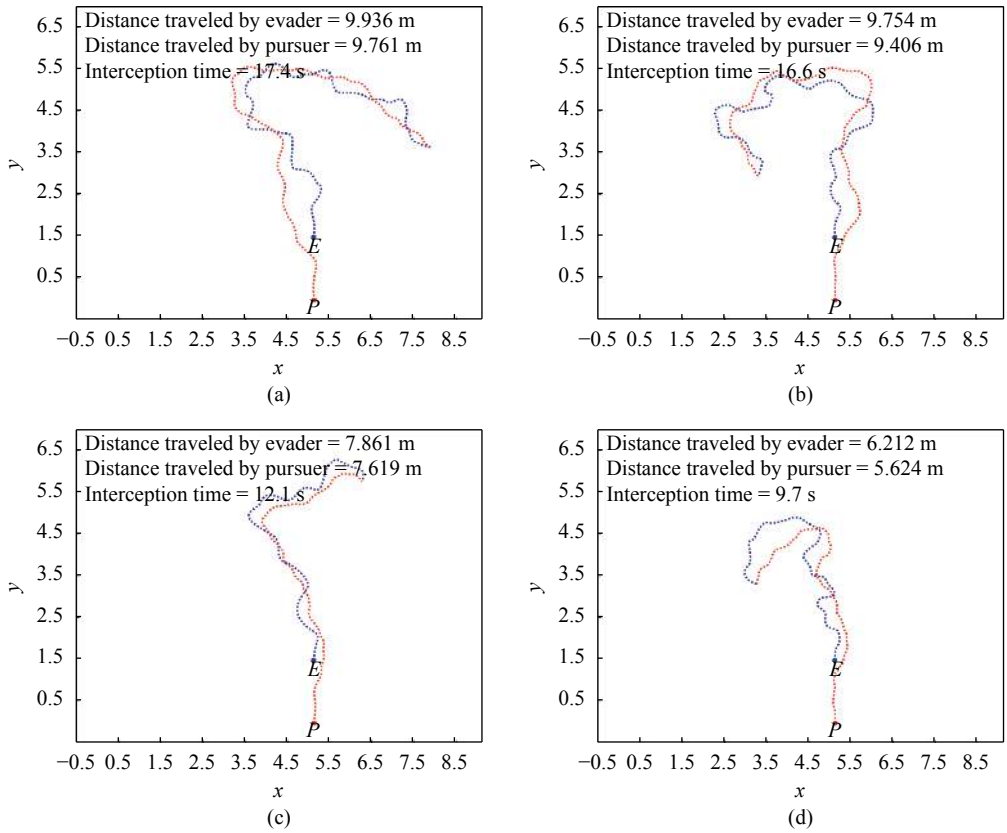

Fig. 11 Interception performance of different pursuer-centric schemes: (a) AIPNG; (b) AAG; (c) Modified AIPNG; (d) Anticipated trajectory based PNG. The evader is guided by the random motion evasion scheme.

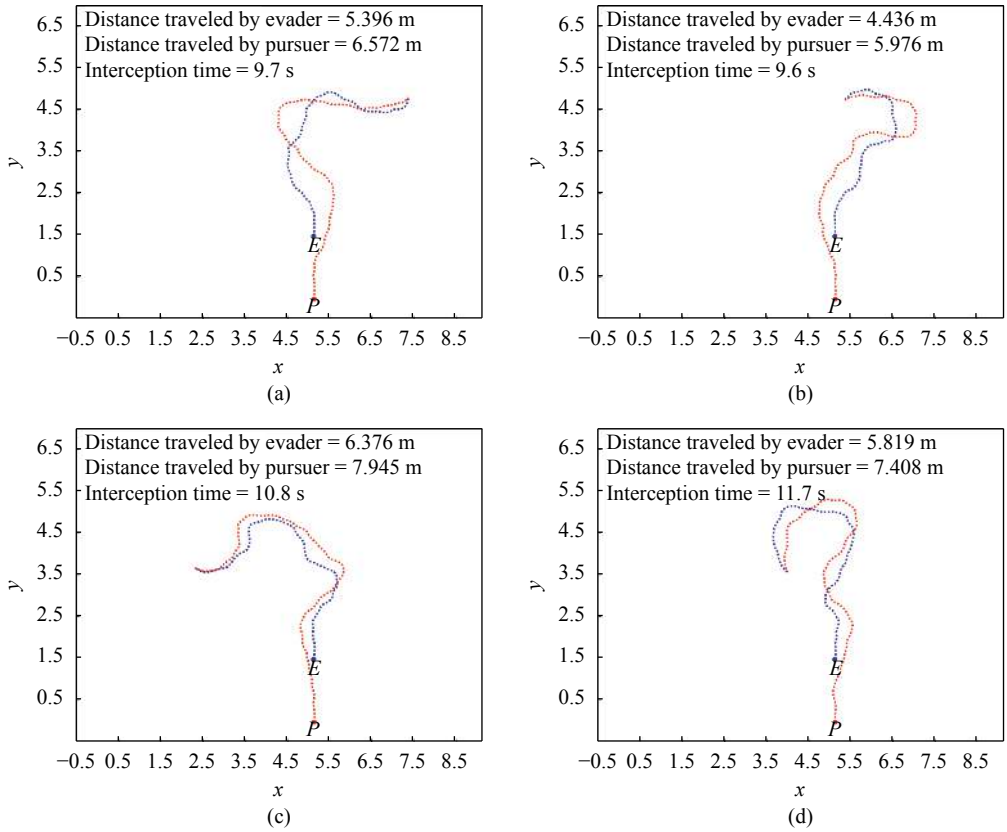

Fig. 12 Interception performance of different pursuer-centric schemes: (a) AIPNG; (b) AAG; (c) Modified AIPNG; (d) Anticipated trajectory based PNG. The evader is guided by the optical-flow based evasion scheme.

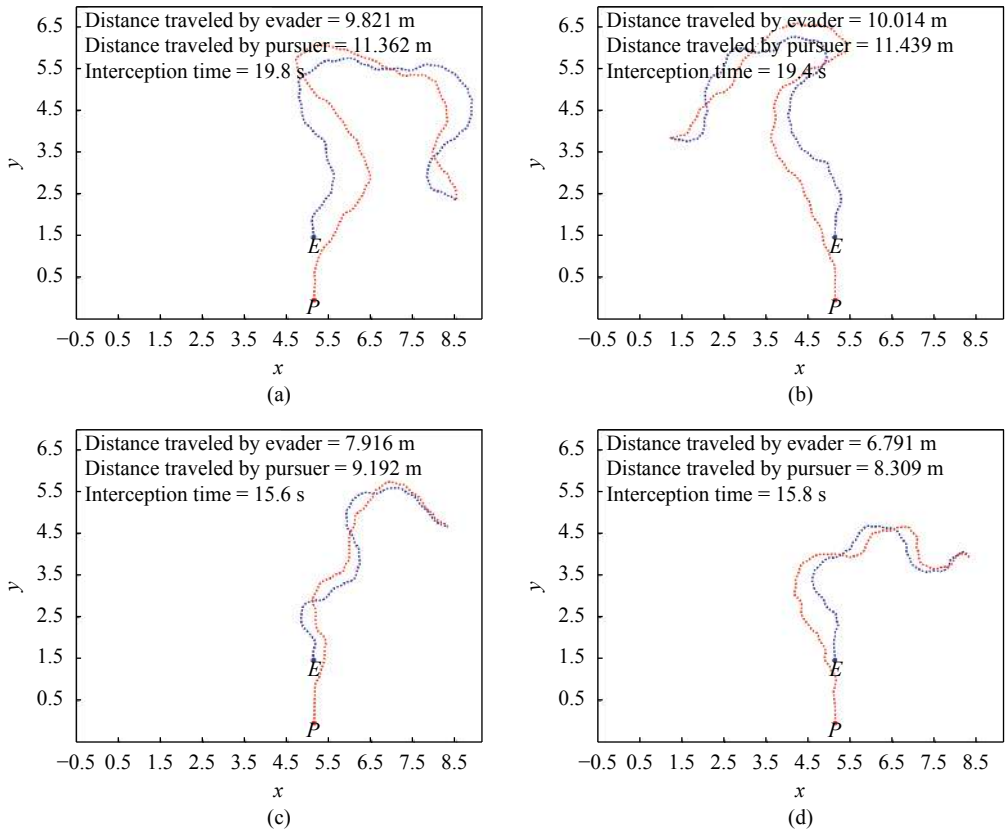

Fig. 13 Interception performance of different pursuer-centric schemes: (a) AIPNG; (b) AAG; (c) Modified AIPNG; (d) Anticipated trajectory based PNG. The evader is guided by the Apollonius circle based evasion scheme.

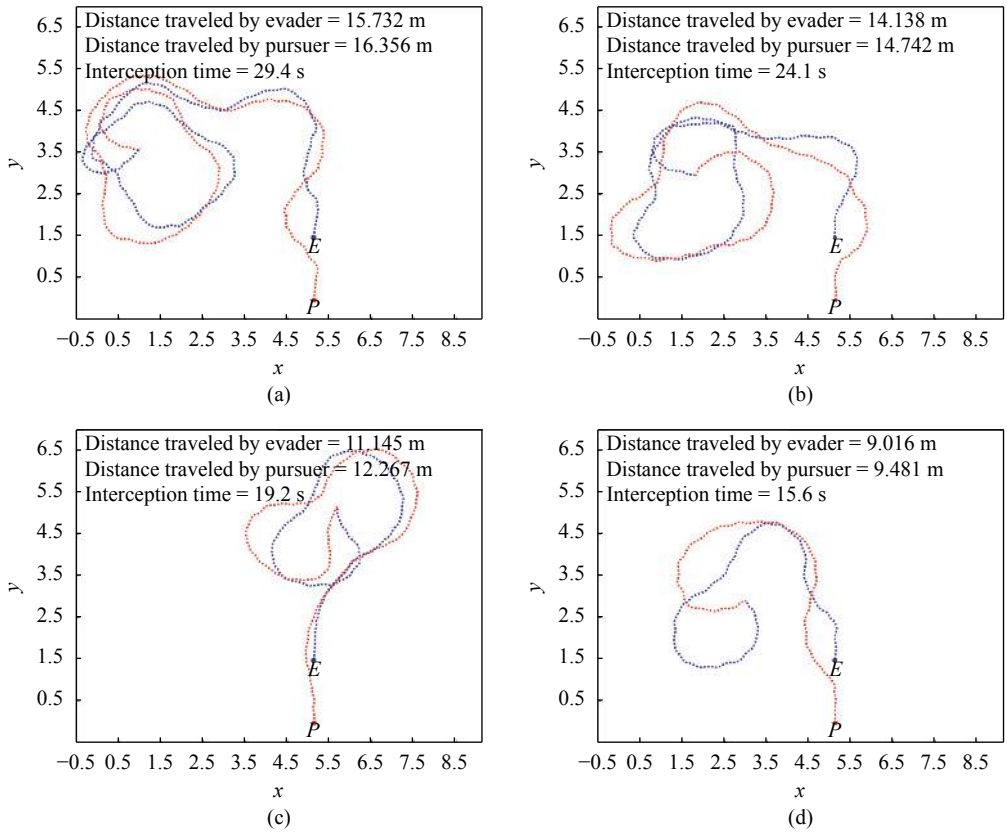

Fig. 14 Interception performance of different pursuer-centric schemes: (a) AIPNG; (b) AAG; (c) Modified AIPNG; (d) Anticipated trajectory based PNG. The evader is guided by the anticipated velocity based evasion scheme.

much as possible.

It can be concluded that the anticipated velocity-based evasion strategy outperforms all the other investigated evasion strategies. Random motion and Apollonius circle based evasion strategies also perform well when the pursuer is guided either by the AIPNG or AAG scheme. On the other hand, AIPNG and AAG pursuer-centric schemes perform satisfactorily against classic and optical-flow based evasion schemes, while modified AIPNG and anticipated trajectory based PNG schemes demonstrate remarkable performance against the random motion, Apollonius circle and anticipated velocity based evasion

Table 4 Student t-test results for distance travelled by the evader using different evasion schemes when the pursuer is guided by the AIPNG scheme

Pursuer's scheme	Evader's scheme		Mean of distance traveled by Evasion scheme 1	Variance of distance traveled by Evasion scheme 1	Mean of distance traveled by Evasion scheme 2	Variance of distance traveled by Evasion scheme 2	t-value
	Evasion scheme 1	Evasion scheme 2					
AIPNG	Classic	Random motion	6.419	24.271	11.384	19.082	**2.87**
		Optical flow	6.419	24.271	6.618	23.196	0.17
		Apollonius circle	6.419	24.271	11.318	22.471	**2.81**
		Anticipated velocity	6.419	24.271	17.191	22.693	**4.79**
	Random motion	Optical flow	11.384	19.082	6.618	23.196	**2.76**
		Apollonius circle	11.384	19.082	11.318	22.471	0.07
		Anticipated velocity	11.384	19.082	16.391	22.693	**2.91**
	Optical flow	Apollonius circle	6.618	23.196	11.318	22.471	**2.64**
		Anticipated velocity	6.618	23.196	16.391	22.693	**4.58**
	Apollonius circle	Anticipated velocity	11.318	22.471	16.391	22.693	**2.84**

schemes.

All the experimental results are also validated by the student t-test. Distance traveled in each scheme has been considered in this statistical test. Interception time is proportional to the distance traversed by the players. Table 4 shows results of the student t-test results for all possible pairs of evasion schemes when the pursuer is guided by the AIPNG scheme. Eight sample paths were taken to compute the mean and variance. Value of $\delta = 1.3$ and $ini\_dis \in \{1.5,\ 2,\ 2.5,\ 3\}$ have been taken for statistical validation of the results. These results can be interpreted as, e.g., the mean value of the distance traveled by the evader in random motion scheme is significantly greater than that of classic evasion and the computed t-value is greater than 2.14. This ascertains 95% statistical correctness that the random motion evasion strategy outperforms the classic evasion strategy when the pursuer is guided by the AIPNG scheme. There is no claim on the performance difference when the t-value is less than 2.14 because the critical t-value is taken as 2.14 in a standard student t-test to ascertain 95% statistical correctness when the number of samples is eight. Tables 5–7 show student t-test results performed on all possible pairs of five evasion schemes against AAG, modified AIPNG and anticipated trajectory-based PNG schemes, respectively. Tables 8–12 show t-test results which have been performed on all possible pairs of pursuer-centric schemes when the evader is guided by classic, random motion, optical-flow, Apollonius circle and anticipated velocity-based evasion schemes, respectively.

6 Conclusions

The present work focuses on performance evaluation of some of the recent pursuer-centric and evader-centric techniques in pursuit-evasion games involving wheeled mobile robots. Four proportional navigation based schemes AIPNG, modified AIPNG, AAG and a recently

Table 5 Student t-test results for distance travelled by the evader using different evasion schemes when the pursuer is guided by the AAG scheme

Pursuer's scheme	Evader's scheme		Mean of distance traveled by Evasion scheme 1	Variance of distance traveled by Evasion scheme 1	Mean of distance traveled by Evasion scheme 2	Variance of distance traveled by Evasion scheme 2	t-value
	Evasion scheme 1	Evasion scheme 2					
AAG	Classic	Random motion	5.755	18.394	11.268	19.273	**3.01**
		Optical flow	5.755	18.394	5.691	20.841	0.06
		Apollonius circle	5.755	18.394	11.626	26.415	**3.31**
		Anticipated velocity	5.755	18.392	15.825	22.271	**4.92**
	Random motion	Optical flow	11.268	19.276	5.691	20.842	**3.14**
		Apollonius circle	11.268	19.273	11.629	26.416	0.26
		Anticipated velocity	11.268	19.278	15.827	22.271	**2.83**
	Optical flow	Apollonius circle	5.691	20.847	11.628	26.415	**2.89**
		Anticipated velocity	5.691	20.846	15.827	22.272	**4.86**
	Apollonius circle	Anticipated velocity	11.629	26.416	15.825	22.271	**2.79**

Table 6 Student t-test results for distance travelled by the evader using different evasion schemes when the pursuer is guided by the modified AIPNG scheme

Pursuer's scheme	Evader's scheme		Mean of distance traveled by Evasion scheme 1	Variance of distance traveled by Evasion scheme 1	Mean of distance traveled by Evasion scheme 2	Variance of distance traveled by Evasion scheme 2	t-value
	Evasion scheme 1	Evasion scheme 2					
Modified AIPNG	Classic	Random motion	6.518	17.421	9.376	20.538	1.89
		Optical flow	6.518	17.421	8.096	19.429	1.13
		Apollonius circle	6.518	17.421	9.427	22.326	1.96
		Anticipated velocity	6.518	17.421	12.894	21.372	**3.04**
	Random motion	Optical flow	9.376	20.538	8.096	19.429	0.91
		Apollonius circle	9.376	20.538	9.427	22.326	0.06
		Anticipated velocity	9.376	20.538	12.894	21.372	**2.21**
	Optical flow	Apollonius circle	8.096	19.429	9.427	22.326	0.98
		Anticipated velocity	8.096	19.429	12.894	21.372	**2.78**
	Apollonius circle	Anticipated velocity	9.427	22.326	12.894	21.372	**2.26**

Table 7 Student t-test results for distance travelled by the evader using different evasion schemes when the pursuer is guided by the ATPNG scheme

Pursuer's scheme	Evader's scheme		Mean of distance traveled by Evasion scheme 1	Variance of distance traveled by Evasion scheme 1	Mean of distance traveled by Evasion scheme 2	Variance of distance traveled by Evasion scheme 2	t-value
	Evasion scheme 1	Evasion scheme 2					
ATPNG	Classic	Random motion	6.318	21.109	7.634	19.832	0.87
		Optical flow	6.318	21.109	6.947	25.046	0.59
		Apollonius circle	6.318	21.109	8.019	17.471	1.19
		Anticipated velocity	6.318	21.109	10.614	19.493	**2.43**
	Random motion	Optical flow	7.634	19.832	6.947	25.046	0.67
		Apollonius circle	7.634	19.832	8.019	17.471	0.33
		Anticipated velocity	7.634	19.832	10.614	19.493	**2.19**
	Optical flow	Apollonius circle	6.947	25.046	8.019	17.471	0.83
		Anticipated velocity	6.947	25.046	10.614	19.493	**2.24**
	Apollonius circle	Anticipated velocity	8.019	17.471	10.614	19.493	1.64

Table 8 Student t-test results for distance travelled by the pursuer using different pursuit strategies when the evader is using classical evasion scheme

Evader's scheme	Pursuer's scheme		Mean of distance traveled by Pursuer scheme 1	Variance of distance traveled by Pursuer scheme 1	Mean of distance traveled by Pursuer scheme 2	Variance of distance traveled by Pursuer scheme 2	t-value
	Pursuer scheme 1	Pursuer scheme 2					
Classical	AIPNG	AAG	7.647	18.493	7.257	22.046	0.30
		Modified AIPNG	7.647	18.493	8.651	21.264	0.83
		Anticipated trajectory	7.647	18.493	8.491	22.649	0.76
	AAG	Modified AIPNG	7.257	22.046	8.651	21.264	1.13
		Anticipated trajectory	7.257	22.046	8.491	22.649	1.04
	Modified AIPNG	Anticipated trajectory	8.651	21.264	8.491	22.649	0.16

Table 9 Student t-test results for distance travelled by the pursuer using different pursuit strategies when the evader is using random motion evasion scheme

Evader's scheme	Pursuer's scheme		Mean of distance traveled by Pursuer scheme 1	Variance of distance traveled by Pursuer scheme 1	Mean of distance traveled by Pursuer scheme 2	Variance of distance traveled by Pursuer scheme 2	t-value
	Pursuer scheme 1	Pursuer scheme 2					
Random motion	AIPNG	AAG	11.047	23.713	10.884	23.285	0.18
		Modified AIPNG	11.047	23.713	8.973	20.457	1.57
		Anticipated trajectory	11.047	23.713	6.823	21.716	**2.87**
	AAG	Modified AIPNG	10.884	23.285	8.973	20.457	1.51
		Anticipated trajectory	10.884	23.285	6.823	21.716	**2.82**
	Modified AIPNG	Anticipated trajectory	8.973	20.457	6.823	21.716	1.65

proposed ATPNG are compared and evaluated against five evader-centric schemes namely, classic evasion, random motion, optical-flow, Apollonius circle and anticipated velocity based evasion. The performance of each of the above mentioned evader-centric schemes has also been evaluated against the pursuer-centric schemes. For the study, two-wheeled mobile robots of the same configuration are taken and all the algorithms are burnt on the Arduino boards of these robots. Performance of each of the schemes is evaluated in terms of interception time and distance traveled by players. Taking the same initial positions for the pursuer and the evader, distance

Table 10 Student t-test results for distance travelled by the pursuer using different pursuit strategies when the evader is using optical-flow evasion scheme

Evader's scheme	Pursuer's scheme		Mean of distance traveled by Pursuer scheme 1	Variance of distance traveled by Pursuer scheme 1	Mean of distance traveled by Pursuer scheme 2	Variance of distance traveled by Pursuer scheme 2	t-value
	Pursuer scheme 1	Pursuer scheme 2					
Optical flow	AIPNG	AAG	7.627	21.925	6.894	23.026	0.56
		Modified AIPNG	7.627	21.925	9.372	20.468	1.37
		Anticipated trajectory	7.627	21.925	9.158	22.457	1.23
	AAG	Modified AIPNG	6.894	23.026	9.372	20.468	1.82
		Anticipated trajectory	6.894	23.026	9.158	22.457	1.68
	Modified AIPNG	Anticipated trajectory	9.372	20.468	9.158	22.457	0.23

Table 11 Student t-test results for distance travelled by the pursuer using different pursuit strategies when the evader is using Apollonius circle evasion scheme

Evader's scheme	Pursuer's scheme		Mean of distance traveled by Pursuer scheme 1	Variance of distance traveled by Pursuer scheme 1	Mean of distance traveled by Pursuer scheme 2	Variance of distance traveled by Pursuer scheme 2	t-value
	Pursuer scheme 1	Pursuer scheme 2					
Apollonius circle	AIPNG	AAG	12.957	23.872	12.871	23.485	0.10
		Modified AIPNG	12.957	23.872	10.657	22.946	1.68
		Anticipated trajectory	12.957	23.872	9.628	21.237	**2.38**
	AAG	Modified AIPNG	12.871	23.485	10.657	22.946	1.64
		Anticipated trajectory	12.871	23.485	9.628	21.237	**2.31**
	Modified AIPNG	Anticipated trajectory	10.657	22.946	9.628	21.237	0.82

Table 12 Student t-test results for distance travelled by the pursuer using different pursuit strategies when the evader is using anticipated velocity based evasion scheme

Evader's scheme	Pursuer's scheme		Mean of distance traveled by Pursuer scheme 1	Variance of distance traveled by Pursuer scheme 1	Mean of distance traveled by Pursuer scheme 2	Variance of distance traveled by Pursuer scheme 2	t-value
	Pursuer scheme 1	Pursuer scheme 2					
Anticipated velocity	AIPNG	AAG	17.583	21.054	16.226	23.479	0.83
		Modified AIPNG	17.583	21.054	13.349	19.751	**2.96**
		Anticipated trajectory	17.583	21.054	10.973	22.861	**4.08**
	AAG	Modified AIPNG	16.226	23.479	13.349	19.751	**2.18**
		Anticipated trajectory	16.226	23.479	10.973	22.861	**3.43**
	Modified AIPNG	Anticipated trajectory	13.349	19.751	10.973	22.861	1.89

traveled by the pursuer equipped with each of the pursuit-strategy is recorded along with the time taken an interception. The same experiment is performed for the five selected evasion strategies. The experiments are repeated with varying initial distances. The path followed by each of the players is also recorded. Based on these observations and the results of student t-tests applied on the data, the following conclusions are made about the pursuer and the evader-centric schemes.

Pursuit strategies

When the evader is guided by random motion or Apollonius circle or anticipated velocity: The ATPNG scheme outperforms all the pursuer-centric schemes. Further, the performance of the AIPNG and AAG schemes

are similar, and the modified AIPNG performs slightly better than the AIPNG and AAG.

When the evader guided by classic or optical-flow: Performance of modified AIPNG and ATPNG schemes are nearly the same. The AIPNG and AAG also exhibit slightly better performance than the modified AIPNG and ATPNG scheme but the results are not statistically significant.

Evasion strategies

When the pursuer guided by AIPNG or AAG: Anticipated velocity based evasion scheme outperforms all the evasion schemes. The performance of the random motion and Apollonius circle based evasion schemes are similar, and are found to be better than the classic and optical-flow based evasion schemes, but the anticipated velocity based evasion shows the best performance.

When the pursuer guided by modified AIPNG or ATPNG: The anticipated velocity-based evasion scheme performs better than the classic and optical-flow. The scheme also performs better than the random motion and Apollonius circle-based evasion schemes but the results are not statistically significant. The optical-flow based evasion performs slightly better than the classic evasion. The performance of the random motion and Apollonius circle scheme are nearly the same and also found to be better than the classic and optical-flow based schemes. However, the results are not found to be statistically significant, based on the student t-test.

Table A1 Interception performance of the players when the evader is guided by five different evasion schemes and the pursuer is guided by the AIPNG scheme

Pursuer's scheme	Initial distance between players (m)	Classic evasion	Random motion evasion	Optical-flow based evasion	Apollonius circle based evasion	Anticipated velocity based evasion
AIPNG	1.5	5.282	9.936	5.396	9.821	15.732
		6.696	9.761	6.572	11.362	16.356
		9.8	**17.4**	**9.7**	**19.8**	**29.4**
	2	6.367	11.383	6.839	11.626	16.517
		7.821	11.429	8.014	13.119	16.719
		11.4	**20.8**	**11.9**	**22.7**	**30.1**
	2.5	7.724	12.624	8.338	13.304	17.692
		9.336	12.581	9.531	14.726	17.991
		13.7	**22.7**	**14.1**	**25.3**	**32.6**
	3	9.308	14.347	10.125	14.726	18.836
		10.982	14.764	11.396	16.083	19.335
		16.3	**26.3**	**17.0**	**27.1**	**33.8**

Table A2 Interception performance of the players when the evader is guided by five different evasion schemes and the pursuer is guided by the AAG scheme

Pursuer's scheme	Initial distance between players (m)	Classic evasion	Random motion evasion	Optical-flow based evasion	Apollonius circle based evasion	Anticipated velocity based evasion
AAG	1.5	4.782	9.754	4.436	10.014	14.138
		5.936	9.406	5.976	11.439	14.742
		9.3	**16.6**	**9.6**	**19.4**	**24.1**
	2	5.918	11.064	6.103	11.794	15.389
		7.236	10.983	7.684	12.908	16.043
		10.8	**18.9**	**11.5**	**22.4**	**25.3**
	2.5	7.197	12.561	7.716	13.084	16.837
		8.496	12.731	9.381	14.318	17.608
		13.3	**22.1**	**14.6**	**24.2**	**27.1**
	3	8.837	14.039	9.461	14.826	18.165
		10.046	14.518	10.946	16.009	19.174
		15.4	**26.8**	**16.2**	**27.8**	**30.8**

Table A3 Interception performance of the players when the evader is guided by five different evasion schemes and the pursuer is guided by the modified AIPNG scheme

Pursuer's scheme	Initial distance between players (m)	Classic evasion	Random motion evasion	Optical-flow based evasion	Apollonius circle based evasion	Anticipated velocity based evasion
Modified AIPNG	1.5	5.563	7.861	6.376	7.916	11.145
		7.082	7.619	7.945	9.192	12.267
		9.0	**12.1**	**10.8**	**15.6**	**19.2**
	2	6.842	9.367	7.691	9.265	12.718
		8.516	9.039	9.264	10.567	13.426
		10.7	**14.8**	**12.1**	**17.8**	**21.6**
	2.5	8.093	10.917	9.046	10.827	14.338
		9.917	10.841	10.718	12.183	15.104
		13.6	**18.4**	**15.2**	**20.1**	**24.4**
	3	9.537	12.538	10.627	12.474	16.038
		11.726	12.387	12.439	13.706	16.846
		15.1	**21.5**	**17.5**	**23.1**	**26.9**

Table A4 Interception performance of the players when the evader is guided by five different evasion schemes and the pursuer is guided by the ATPNG scheme

Pursuer's scheme	Initial distance between players (m)	Classic evasion	Random motion evasion	Optical-flow based evasion	Apollonius circle based evasion	Anticipated velocity based evasion
ATPNG	1.5	5.183	6.212	5.819	6.791	9.016
		6.804	5.624	7.408	8.309	9.481
		10.9	**9.7**	**11.7**	**15.8**	**15.6**
	2	6.509	7.816	7.083	8.194	10.693
		8.264	6.986	8.737	9.906	11.036
		12.1	**11.9**	**13.0**	**17.2**	**18.2**
	2.5	8.178	9.413	8.726	9.916	12.186
		9.965	8.348	10.545	11.663	12.817
		14.2	**14.3**	**14.6**	**19.8**	**20.7**
	3	9.759	11.237	10.265	11.729	13.953
		11.588	10.174	12.038	13.326	14.457
		16.7	**18.1**	**17.8**	**22.4**	**23.6**

Appendix

Table A1 shows the interception performance of the AIPNG pursuer-centric scheme against each of the evader-centric schemes for the value of $\delta = 1.3$ and $ini\_dis \in \{1.5,\ 2,\ 2.5,\ 3\}$. Likewise, Tables A2–A4 show the performance of AAG, modified AIPNG and ATPNG pursuer-centric schemes against all evader-centric schemes, respectively. In all tables, italic and normal font values represent the distance traveled by the evader and the pursuer robots, respectively, while the bold face value represents the interception time.

References

[1] T. H. Chung, G. A. Hollinger, V. Isler. Search and pursuit-evasion in mobile robotics: A survey. *Autonomous Robots*, vol. 31, no. 4, pp. 299–316, 2011. DOI: 10.1007/s10514-011-9241-4.

[2] Y. Song, S. X. Li, C. F. Zhu, H. X. Chang. Object tracking with dual field-of-view switching in aerial videos. *International Journal of Automation and Computing*, vol. 13, no. 6, pp. 565–573, 2016. DOI: 10.1007/s11633-016-0949-7.

[3] B. Das, B. Subudhi, B. B. Pati. Cooperative formation control of autonomous underwater vehicles: An overview. *International Journal of Automation and Computing*, vol. 13, no. 3, pp. 199–225, 2016. DOI: 10.1007/s11633-016-1004-4.

[4] R. Vidal, S. Rashid, C. Sharp, O. Shakernia, J. Kim, S. Sastry. Pursuit-evasion games with unmanned ground and aerial vehicles. In *Proceedings of IEEE International Conference on Robotics and Automation*, Seoul, South Korea, pp. 2948–2955, 2001. DOI: 10.1109/ROBOT.2001.933069.

[5] J. R. Britnell, M. Wildon. Finding a princess in a palace: A pursuit-evasion problem. *The Electronic Journal of Combinatorics*, vol. 20, no. 1, Article number 25, 2013.

[6] B. K. Sahu, B. Subudhi. Adaptive tracking control of an autonomous underwater vehicle. *International Journal of Automation and Computing*, vol. 11, no. 3, pp. 299–307, 2014. DOI: 10.1007/s11633-014-0792-7.

[7] X. X. Sun, W. Yeoh, S. Koenig. Moving target D* lite*. In *Proceedings of the 9th International Conference on Autonomous Agents and Multiagent Systems*, ACM, Toronto, Canada, pp. 67–74, 2010. DOI: 10.1145/1838206.1838216.

[8] N. Basilico, N. Gatti, F. Amigoni. Patrolling security games: Definition and algorithms for solving large instances with single patroller and single intruder. *Artificial Intelligence*, vol. 184–185, pp. 78–123, 2012. DOI: 10.1016/j.artint.2012.03.003.

[9] L. Freda, G. Oriolo. Vision-based interception of a moving target with a nonholonomic mobile robot. *Robotics and Autonomous Systems*, vol. 55, no. 6, pp. 419–432, 2007. DOI: 10.1016/j.robot.2007.02.001.

[10] Y. Tian, Y. Li, Z. Ren. Vision-based adaptive guidance law for intercepting a manoeuvring target. *IET Control Theory & Applications*, vol. 5, no. 3, pp. 421–428, 2011. DOI: 10.1049/iet-cta.2010.0092.

[11] J. P. Hwang, J. Baek, B. Choi, E. Kim. A novel part-based approach to mean-shift algorithm for visual tracking. *International Journal of Control, Automation and Systems*, vol. 13, no. 2, pp. 443–453, 2015. DOI: 10.1007/s12555-013-0483-0.

[12] R. J. Wai, Y. W. Lin. Adaptive moving-target tracking control of a vision-based mobile robot via a dynamic petri recurrent fuzzy neural network. *IEEE Transactions on Fuzzy Systems*, vol. 21, no. 4, pp. 688–701, 2013. DOI: 10.1109/TFUZZ.2012.2227974.

[13] A. M. Rao, K. Ramji, B. S. K. Sundara Siva Rao, V. Vasu, C. Puneeth. Navigation of non-holonomic mobile robot using neuro-fuzzy logic with integrated safe boundary algorithm. *International Journal of Automation and Computing*, vol. 14, no. 3, pp. 285–294, 2017. DOI: 10.1007/s11633-016-1042-y.

[14] Q. C. Li, W. S. Zhang, G. Han, Y. H. Zhang. Finite time convergent wavelet neural network sliding mode control guidance law with impact angle constraint. *International Journal of Automation and Computing*, vol. 12, no. 6, pp. 588–599, 2015. DOI: 10.1007/s11633-015-0927-5.

[15] L. Q. Li, W. X. Xie. Bearings-only maneuvering target tracking based on fuzzy clustering in a cluttered environment. *AEU – International Journal of Electronics and Communications*, vol. 68, no. 2, pp. 130–137, 2014. DOI: 10.1016/j.aeue.2013.07.013.

[16] M. H. Amoozgar, S. H. Sadati, K. Alipour. Trajectory tracking of wheeled mobile robots using a kinematical fuzzy controller. *International Journal of Robotics and Automation*, vol. 27, no. 6, pp. 49–59, 2012. DOI: 10.2316/Journal.206.2012.1.206-3476.

[17] N. Duan, H. F. Min. NN-based output tracking for more general stochastic nonlinear systems with unknown control coefficients. *International Journal of Automation and Computing*, vol. 14, no. 3, pp. 350–359, 2017. DOI: 10.1007/s11633-015-0936-4.

[18] F. Belkhouche, B. Belkhouche, P. Rastgoufard. Line of sight robot navigation toward a moving goal. *IEEE Transactions on Systems, Man, and Cybernetics, Part B* (*Cybernetics*), vol. 36, no. 2, pp. 255–267, 2006. DOI: 10.1109/TSMCB.2005.856142.

[19] C. Z. Zhao, Y. Huang. ADRC based integrated guidance and control scheme for the interception of maneuvering targets with desired LOS angle. In *Proceedings of the 29th Chinese Control Conference*, Beijing, China, pp. 6192–6196, 2010.

[20] H. M. Prasanna, D. Ghose. Retro-proportional-navigation: A new guidance law for interception of high speed targets. *Journal of Guidance, Control, and Dynamics*, vol. 35, no. 2, pp. 377–386, 2012. DOI: 10.2514/1.54892.

[21] L. Yan, J. G. Zhao, H. R. Shen, Y. Li. Biased retro-proportional navigation law for interception of high-speed targets with angular constraint. *Defence Technology*, vol. 10, no. 1, pp. 60–65, 2014. DOI: 10.1016/j.dt.2013.12.010.

[22] C. H. Lee, T. H. Kim, M. J. Tahk. Biased PNG for target observability enhancement against nonmaneuvering targets. *IEEE Transactions on Aerospace and Electronic Systems*, vol. 51, no. 1, pp. 2–17, 2015. DOI: 10.1109/TAES.2014.120103.

[23] Y. Li, L. Yan, J. G. Zhao, F. Liu, T. Wang. Combined proportional navigation law for interception of high-speed targets. *Defence Technology*, vol. 10, no. 3, pp. 298–303, 2014. DOI: 10.1016/j.dt.2014.07.004.

[24] D. Ghose. True proportional navigation with maneuvering target. *IEEE Transactions on Aerospace and Electronic Systems*, vol. 30, no. 1, pp. 229–237, 1994. DOI: 10.1109/7.250423.

[25] C. D. Yang, C. C. Yang. Optimal pure proportional navigation for maneuvering targets. *IEEE Transactions on Aerospace and Electronic Systems*, vol. 33, no. 3, pp. 949–957, 1997. DOI: 10.1109/7.599315.

[26] M. Mehrandezh, M. N. Sela, R. G. Fenton, B. Benhabib. Robotic interception of moving objects using ideal proportional navigation guidance technique. *Robotics and Autonomous Systems*, vol. 28, no. 4, pp. 295–310, 1999. DOI: 10.1016/S0921-8890(99)00044-5.

[27] M. Mehrandezh, M. N. Sela, R. G. Fenton, B. Benhabib. Robotic interception of moving objects using an augmented ideal proportional navigation guidance technique. *IEEE Transactions on Systems, Man, and Cybernetics-Part A: Systems and Humans*, vol. 30, no. 3, pp. 238–250, 2000. DOI: 10.1109/3468.844351.

[28] J. L. Gu, W. C. Chen. Optimal proportional navigation guidance based on generalized predictive control. In *Proceedings of the 16th International Conference on System Theory, Control and Computing*, Sinaia, Romania, 2012.

[29] M. Keshmiri, M. Keshmiri. Performance comparison of various navigation guidance methods in interception of a moving object by a serial manipulator considering its kinematic and dynamic limits. In *Proceedings of the 15th International Conference on Methods and Models in Automation and Robotics*, Miedzyzdroje, Poland, pp. 212–217, 2010. DOI: 10.1109/MMAR.2010.5587234.

[30] Y. Y. Song, W. C. Chen, X. L. Yin. A new angular acceleration guidance law with estimation approach based on sliding mode observer against high maneuvering target. *Applied Mechanics and Materials*, vol. 110–116, pp. 5249–5256, 2012. DOI: 10.4028/www.scientific.net/AMM.110-116.5249.

[31] A. Kumar, A. Ojha, P. K. Padhy. Anticipated trajectory based proportional navigation guidance scheme for intercepting high maneuvering targets. *International Journal of Control, Automation and Systems*, vol. 15, no. 3, pp. 1351–1361, 2017. DOI: 10.1007/s12555-015-0166-0.

[32] S. Kim, H. J. Kim. Robust proportional navigation guidance against highly maneuvering targets. In *Proceedings of the 13th International Conference on Control, Automation and Systems*, Gwangju, South Korea, pp. 61–65, 2013.

DOI: 10.1109/ICCAS.2013.6703864.

[33] S. Ghosh, D. Ghose, S. Raha. Capturability of augmented pure proportional navigation guidance against time-varying target maneuvers. *Journal of Guidance, Control, and Dynamics*, vol. 37, no. 5, pp. 1446–1461, 2014. DOI: 10.2514/1.G000561.

[34] R. Isaacs. *Differential Games: A Mathematical Theory with Applications to Warfare and Pursuit, Control and Optimization*, New York, USA: John Wiley and Sons, 1965.

[35] P. A. Meschler. On constructing efficient evasion strategies for a game with imperfect information. *IEEE Transactions on Automatic Control*, vol. 15, no. 5, pp. 576–580, 1970. DOI: 10.1109/TAC.1970.1099558.

[36] W. Rzymowski. Avoidance of one pursuer. *Journal of Mathematical Analysis and Applications*, vol. 120, no. 1, pp. 89–94, 1986. DOI: 10.1016/0022-247X(86)90206-4.

[37] W. Chodun. Differential games of evasion with many pursuers. *Journal of Mathematical Analysis and Applications*, vol. 142, no. 2, pp. 370–389, 1989. DOI: 10.1016/0022-247X(89)90007-3.

[38] G. I. Ibragimov, M. Salimi, M. Amini. Evasion from many pursuers in simple motion differential game with integral constraints. *European Journal of Operational Research*, vol. 218, no. 2, pp. 505–511, 2012. DOI: 10.1016/j.ejor.2011.11.026.

[39] S. Y. Liu, Z. Y. Zhou, C. Tomlin, K. Hedrick. Evasion as a team against a faster pursuer. In *Proceedings of American Control Conference*, Washington, USA, pp. 5368–5373, 2013. DOI: 10.1109/ACC.2013.6580676.

[40] D. Pais, N. E. Leonard. Pursuit and evasion: Evolutionary dynamics and collective motion. In *Proceedings of AIAA Guidance, Navigation, and Control Conference*, Toronto, Canada, 2010. DOI: 10.2514/6.2010-7584.

[41] M. V. Raman, M. Kothari. Pursuit-evasion games of high speed evader. *Journal of Intelligent & Robotic Systems*, vol. 85, no. 2, pp. 293–306, 2017. DOI: 10.1007/s10846-016-0379-3.

[42] A. Kumar, A. Ojha. Anticipated velocity based guidance strategy for wheeled mobile evader amidst stationary and moving obstacles in bounded environment. *Computer Animation & Virtual Worlds*, vol. 26, no. 5, pp. 495–507, 2015. DOI: 10.1002/cav.1609.

[43] G. Foderaro, A. Swingler, S. Ferrari. A model-based cell decomposition approach to on-line pursuit-evasion path planning and the video game Ms. Pac-Man. In *Proceedings of IEEE Conference on Computational Intelligence and Games*, Granada, Spain, pp. 281–287, 2012. DOI: 10.1109/CIG.2012.6374167.

[44] E. Bakolas. Evasion from a group of pursuers with double integrator kinematics. In *Proceedings of the 52nd IEEE Conference on Decision and Control*, Florence, Italy, pp. 1472–1477, 2013. DOI: 10.1109/CDC.2013.6760090.

[45] B. Li, R. Chiong, L. G. Gong. Search-evasion path planning for submarines using the artificial bee colony algorithm. In *Proceedings of IEEE Congress on Evolutionary Computation*, Beijing, China, pp. 528–535, 2014. DOI: 10.1109/CEC.2014.6900224.

[46] I. Exarchos, P. Tsiotras. An asymmetric version of the two car pursuit-evasion game. In *Proceedings of the 53rd IEEE Conference on Decision and Control*, Los Angeles, USA, pp. 4272–4277, 2014. DOI: 10.1109/CDC.2014.7040055.

[47] J. C. Las Fargeas, P. T. Kabamba, A. R. Girard. Path planning for information acquisition and evasion using marsupial vehicles. In *Proceedings of American Control Conference*, Chicago, USA, pp. 3734–3739, 2015. DOI: 10.1109/ACC.2015.7171910.

[48] W. Sun, P. Tsiotras. Pursuit evasion game of two players under an external flow field. In *Proceedings of American Control Conference*, Chicago, USA, pp. 5617–5622, 2015. DOI: 10.1109/ACC.2015.7172219.

[49] P. J. Yuan, J. S. Chem. Ideal proportional navigation. *Journal of Guidance, Control, and Dynamics*, vol. 15, no. 5, pp. 1161–1165, 1992. DOI: 10.2514/3.20964.

Amit Kumar received the B. Sc. degree in computer science and engineering from Institution of Electronics and Telecommunication Engineers, India in 2008, the M. Tech. and Ph. D. degrees in computer science and engineering from Pandit Dwarka Prasad Mishra (PDPM) Indian Institute of Information Technology Design and Manufacturing Jabalpur, India in 2010 and 2016, respectively. Presently, he is working as an assistant professor in Computer Science and Engineering Department, Indian Institute of Information Technology, India.

His research interests include robot motion planning, deep learning, multi-robot systems.

E-mail: amit@iiitkota.ac.in (Corresponding author)
ORCID iD: 0000-0002-0777-7715

Aparajita Ojha received the Ph. D. degree in mathematics from Rani Durgavati (R. D.) University, India in 1987. She is a professor of computer science and engineering discipline at Indian Institute of Information Technology, Design and Manufacturing Jabalpur, India, and prior to her current position, she was a professor of Mathematics at R. D. University, India.

Her research interests include robotics, computer aided design, geometric modeling, finite elements, spline theory, approximation theory, wavelet analysis, object and aspect oriented modeling.

E-mail: aojha@iiitdmj.ac.in